Journal of
Medicinal Chemistry

Article

Rapid solid phase construction of serine hydrolase probes results in selective activity-based probes for acyl protein thioesterases-1/2

Roeland Vanhoutte, Merel A. T. van de Plassche, and Steven H.L. Verhelst

J. Med. Chem., **Just Accepted Manuscript** • DOI: 10.1021/acs.jmedchem.0c01043 • Publication Date (Web): 29 Sep 2020

Just Accepted

is published by the American Chemical Society. 1155 Sixteenth Street N.W., Washington, DC 20036

Rapid solid phase construction of serine hydrolase probes results in selective activity-based probes for acyl protein thioesterases-1/2

Roeland Vanhoutte,[1] Merel A. T. van de Plassche,[1] and Steven H. L. Verhelst[*, 1,2]

[1] KU Leuven, Department of Cellular and Molecular Medicine, Laboratory of Chemical Biology, Herestr. 49, 3000 Leuven, Belgium

[2] Leibniz Institute for Analytical Sciences ISAS, e.V., Otto-Hahn-Str. 6b, 44227 Dortmund, Germany

* Corresponding author: steven.verhelst@isas.de, steven.verhelst@kuleuven.be

Abstract

Serine hydrolases are a large, diverse family of enzymes that play various biomedically important roles. Their study has been substantially advanced by activity-based protein profiling, which makes use of covalent chemical probes for labeling of the active site and detection by various methodologies. However, highly selective probes for individual serine hydrolases are scarce, because probe synthesis usually takes place by time-consuming solution phase chemistry. We here report a general solid phase synthesis towards serine hydrolase chemical probes, which will speed up probe library synthesis. It involves construction of a recognition element ending in a secondary amine followed by capping with different electrophiles. We illustrate the power of this approach by the discovery of selective chemical probes for the depalmitoylating enzymes APT-1/2. Overall, this study provides new methodologies to synthesize serine hydrolase probes, while providing new reagents to study protein depalmitoylation.

Introduction

Activity-based protein profiling (ABPP) emerged two decades ago to help discover the function of enzymes.[1] ABPP uses small molecules called activity-based probes (ABPs), which bind covalently to the active site of the enzymes of interest, allowing a multitude of read-out possibilities and application areas,[2] including profiling in different disease states, imaging, target identification as well as inhibitor screening by competitive ABPP (Figure 1A). ABPs generally consist of three parts: a warhead, which binds covalently to a catalytic residue of the target enzyme, a recognition element, which influences the selectivity of a probe, and a reporter tag to visualize probe labeled proteins.

Fluorophosphonate (FP) probes (Figure 1B) were developed as the first serine hydrolase reactive ABPs – either equipped with a biotin tag (FP-Biotin)[3] or a fluorophore (FP-rhodamine; FP-Rh).[4,5] Serine hydrolases (SHs) are an enzyme superfamily comprising 1-2% of the human genome. Amongst them are several pharmaceutically interesting proteins,[6] such as monoacyl glycerol lipase (MAGL) and α,β-hydrolase domain containing protein 6 (ABDH6), which play a role in the generation of endocannabinoids in the nervous system,[7] acyl protein thioesterases-1/2 (APT-1/2; previously known as lysophospholipases-1/2; LYPLA-1/2), which are involved in depalmitoylation of Ras GTPase,[8] and protein phosphatase methyl esterase 1, which plays a role in neuroblastoma.[9] For most SH members, however, the exact function remains elusive. Conveniently, FP-Rh reacts with more than 80% of all metabolic SHs in mice.[10] Hence, FP-Rh has not only been useful for the study of well known SHs, but also for uncharacterized ones. However, there are also some limitations of this reagent: (1) The synthesis is not trivial and takes considerable effort. (2) It may not react with all SHs. (3) Because of its general nature, it is problematic to implement this probe in studies for visualization of a single SH of interest. Therefore, serine-reactive ABPs with other warheads and recognition elements have been developed over the past two decades. These have the potential to be used for in vivo imaging studies, as recently illustrated for MAGL.[11, 12] Nevertheless, it is extremely challenging and time-consuming to obtain highly selective ABPs, because the synthesis and optimization of these ABPs usually takes place by solution phase chemistry. Hence, selective SH ABPs have

only been reported for a few SHs, including neutral cholesterol ester hydrolase 1 (KIAA1363),[13] diacylglycerol lipase (DAGL),[14, 15] and MAGL,[16] although probes for the last two showed some crossreactivity towards ABDH6. In order to produce and optimize ABPs in a fast and efficient manner, we set out to speed up the process of SH probe development by applying solid phase synthesis. Here, we present a mix-and-match strategy of recognition elements and serine reactive warheads for the design and full on-resin synthesis of a SH ABP library. Triazole urea probes in this library were potent and selective against APT-1/2, and represent new tools for the study of protein depalmitoylation.

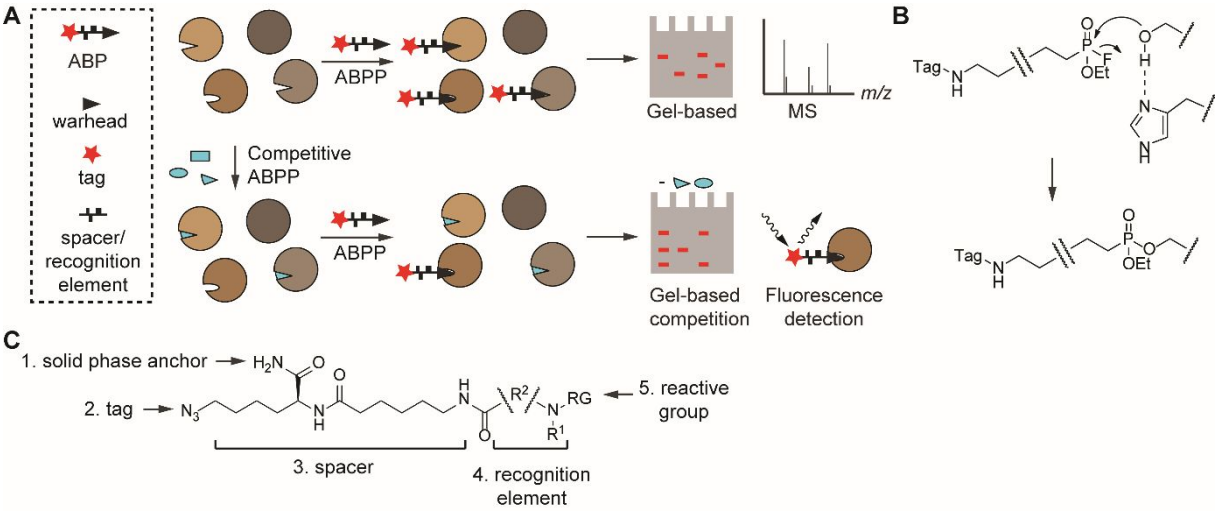

Figure 1. ABPP and ABPs. (A) Left (boxed): ABPs generally consist of three elements: a reactive electrophile as warhead that engages in a mechanism-based reaction with the active site nucleophiles of the target, a tag that allows detection and a spacer and/or recognition element to prevent a steric clash of the tag in the active site and to influence the selectivity of the probe. Right: ABPP allows the tagging of active enzyme targets in a complex proteome, such as a cell lysate, whole cell or in vivo setting, followed by various types of read-out. Inhibitor evaluation in complex proteomes may be done by 'competitive ABPP', in which the proteome is first treated with a potential inhibitor before incubation with the ABP. Disappearance of gel bands in SDS-PAGE will then reveal inhibitor selectivity. (B) Structure of fluorophosphonate-based probes and the mechanism of reaction with serine hydrolases: the active site serine side chain, activated by hydrogen bonding to a histidine residue, engages in a mechanism-based

reaction and results in a stable, covalent phosphonate ester probe-protein complex. (C) A modular design of SH ABPs for construction on solid support.

Results and discussion

Design & synthesis of probes. We aimed at making ABPs for SHs in a time-efficient manner by a full on resin synthesis. Therefore, our probes comprised the following modular design (Figure 1C): (1) a C-terminal amide which forms the anchor to the common Rink amide resin, (2) an azide tag amenable to click chemistry-mediated detection of probe targets and incorporated in (3) an azidolysine-aminohexanoic acid spacer that connects to (4) a recognition element consisting of a natural amino acid, an unnatural amino acid or a peptoid (or a combination thereof), and (5) a serine reactive electrophile. In this design, the reactive group is introduced on resin as an N-terminal cap in the very last step prior to resin cleavage. As warheads, we selected five types of reactive electrophiles (Scheme 1A) which have previously been shown to react with serine hydrolases and that can potentially be installed at an amine in a last step on solid support: a diphenylphosphoramidate,[17] an N-hydroxysuccinimidylcarbamate (NHS carbamate),[16] a (nitro-)phenylcarbamate, a 2-aminopyridineurea[18] and a 1,2,3-triazoleurea.[19] The introduction at this point of the synthesis would minimize the incompatibilty with any used reagents and conditions except for the coupling conditions of the reactive group and the cleavage conditions from the resin. Whereas diphenylphosphoramidates have already been synthesized on resin,[17] this possibility has not yet been explored for the other reactive electrophiles. In a pilot experiment (Scheme 1A), we explored coupling these reactive groups to recognition elements ending in a primary amine (a phenyl alanine), a secondary amine (a phenylalanine peptoid) or a secondary amine in a six-membered ring (an isonipecotic acid). We found that primary amines capped as hydroxysuccinimidylcarbamates converted into hydantoins (Figure S1) and we could not form triazole ureas onto primary or non-cyclic secondary amines. However, all reactive groups could be placed onto the piperidine ring of isonipecotic acid as detected by LC-MS of crude

compound mixtures after resin cleavage (Figure S2). This inspired us to make a series of recognition elements, consisting of a piperidine or piperazine-moiety connected to an additional aromatic group, a combination which has previously shown to have affinity for various serine hydrolases.[19 20 21 22]

Scheme 1. Synthesis of mix-and-match SH ABP libraries.[a]

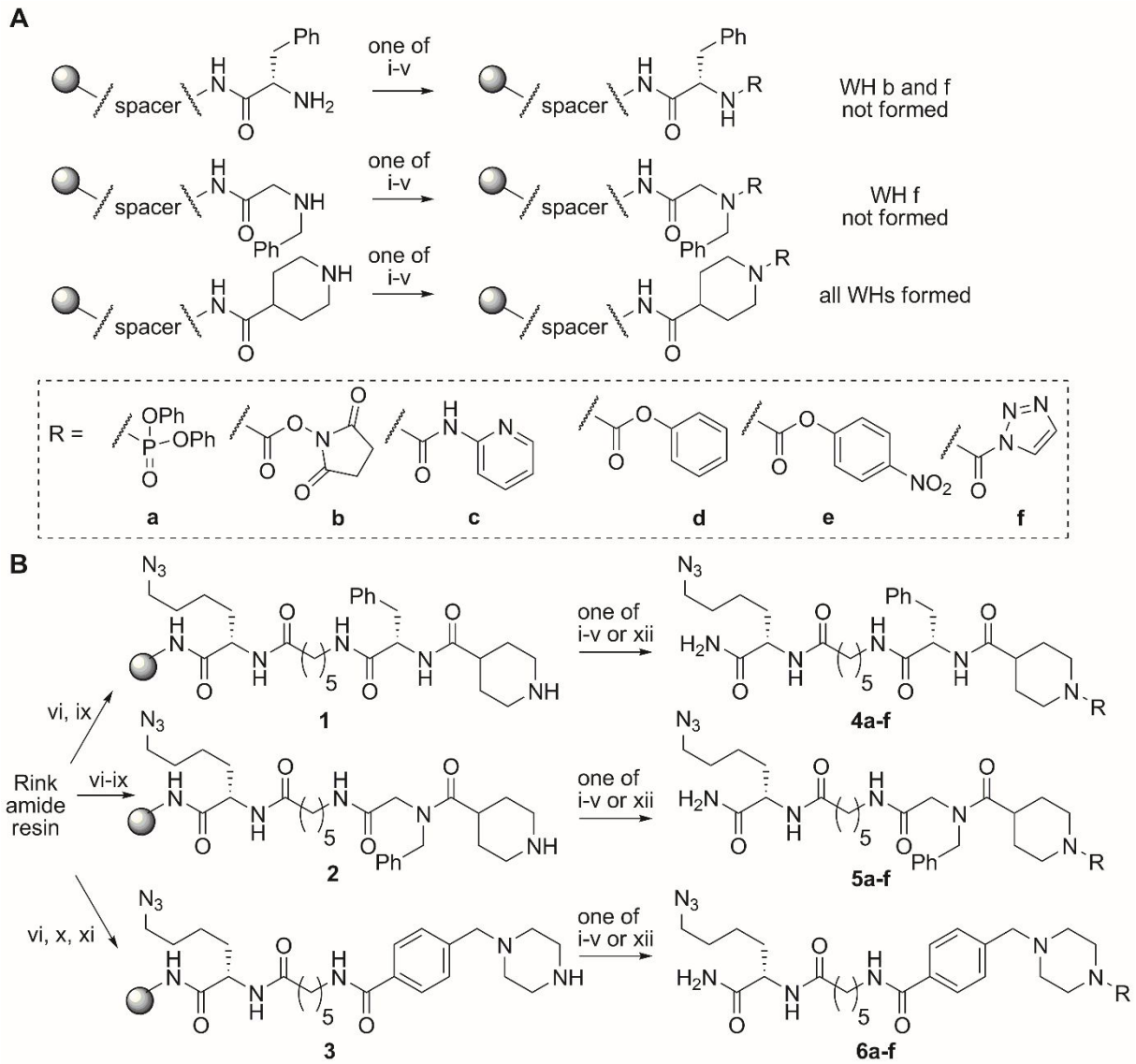

[a] (A) On resin coupling of warheads to different types of amines. *Reagents and conditions*: (i) Diphenylphosphoryl chloride, DIEA, DCM. (ii) Disuccinimidylcarbonate, DIEA, DCM. (iii) 2-aminopyridinyl phenyl carbamate, DIEA, DCM. (iv) phenyl chloroformate, DIEA, DCM. (v) 1. Triphosgene, DIEA, DCM, 30 minutes; 2. 1*H*-1,2,3-triazole, DIEA, DCM. (B) Library synthesis

towards compounds **4a-6f**. (vi) SPPS elongation by 1. DMF/piperidine 4/1, 15 min; 2. Fmoc-aa-OH, HBTU, DIEA, DMF. (vii) 1. DMF/piperidine 4/1, 5 min; 2. Bromoacetic acid, DIC, HOBt, DMF. (viii) Benzylamine, DIEA, DMF. (ix) Fmoc-Inp-OH, DIC, HOBt, DMF. (x) p-Bromomethylbenzoic acid, PyBrOP, DIEA, DMF. (xi) Piperazine, DMF. (xii) 4-nitrophenyl chloroformate, DIEA, DCM.

Library synthesis. The three recognition elements in the probe library (Scheme 1B) comprised of isonipecotic acid coupled to phenylalanine (**1**), isonipecotic acid coupled to a phenylalanine peptoid (**2**), or *para*-piperazinylmethyl benzoic acid (**3**). These recognition elements were synthesized by modified SPPS and installed onto a Lys(N_3)-Ahx click-tag/linker moiety. Specifically, elongation with Phe took place under standard conditions, whereas the peptoid Phe was synthesized by coupling a bromoacetic acid followed by on resin nucleophilic substitution of the bromide by benzylamine. These two recognition elements were completed by coupling of isonipecotic acid (Inp) under influence of DIC/HOBt. The third recognition element was formed by installation of a 4-bromomethylbenzoyl substituent followed by S_N2 substitution with piperazine. All three recognition elements were then capped with six warheads. Gratifyingly, these compounds were all compatible with Rink amide resin cleavage conditions, giving a 3x6 library of ABPs **4a-6f**.

Activity against SHs in competitive ABPP. Next, we set out to test whether these compounds display reactivity against SHs. Mouse brain lysate was chosen as a suitable proteome for screening, because it contains a wide variety of pharmacologically interesting SHs. Previous studies have identified between approximately 25 and 40 different SHs in this lysate and conveniently, the retention of several of these on SDS-PAGE is known..[23 24 25] Hence, the cytosolic and membrane fractions of mouse brain lysates were pretreated with compounds **4a-6f** and residually active SHs were labeled with FP-Rh (Figure 2A). Interestingly, this competitive ABPP experiment revealed that five library members (the three triazole ureas **4f**, **5f** and **6f**, and two NHS-carbamates **5b** and **6b**) showed selective inhibition of two close-

running gel bands that have previously been identified as APT-1/2 (Figure 2A).[26] A titration of these compounds showed that the potency of the NHS carbamates **5b** and **6b** for these targets was moderate (see Figure S3), whereas the triazole ureas were much more potent (low to mid nanomolar range) (Figure 2B, see also Figure S4 for representative gels).

Probe **4f**, with a Phe-Inp recognition element had an apparent IC_{50} of 460 ± 50 nM for APT-1/2. For the other targets of FP-rhodamine, this probe had apparent IC_{50} values above 30 μM (Figure S4), resulting in a larger than 65 fold selectivity. Remarkably, the potency for APT-1/2 increased 37 fold by replacing the Phe in the recognition element by its peptoid analog in **5f** (IC_{50}^{App}= 11.8 ± 1.8 nM) (Figure 2B), while having an excellent selectivity (over 2500 fold, as measured by apparent IC_{50} values against the other FP-Rh targets, which were above 30 μM, see Figure S4). Probe **6f**, with a linear benzyl-piperazinyl recognition element also showed high activity against APT-1/2 (IC_{50}^{App} = 27.9 ± 2.8 nM), although at micromolar concentrations this probe also inhibited ABHD6 (Figure S4) with an apparent IC_{50} of 7.4 ± 1.7 μM (approximately 250 fold selectivity).

We next compared probe **5f** with the chloro-isocoumarin-based probe JCP-174-alk[27] and the isoform selective APT-1 and APT-2 inhibitors ML-348 and ML349.[26] To this end, competitive ABPP was performed in the soluble fraction of mouse brain lysate. We found that the gel bands that are competed with probe **5f** also disappear upon treatment with JCP-174-alk (Figure 2C, left panel). Moreover, inhibitors ML-348 and ML-349 only compete one of the two close-running gel bands inhibited by probe **5f**. Overall, this reveals that **5f** has similar inhibitory capacity and confirms APT-1/2 as target. We assessed the cell permeability of probes **5f** and **6f** using the human squamous carcinoma cell line A431. In a competitive ABPP assay with FP-rhodamine both **5f** and **6f** fully inhibited all active APT-1/2 at 1 μM concentration (Figure 2D), confirming their target engagement in live cells.

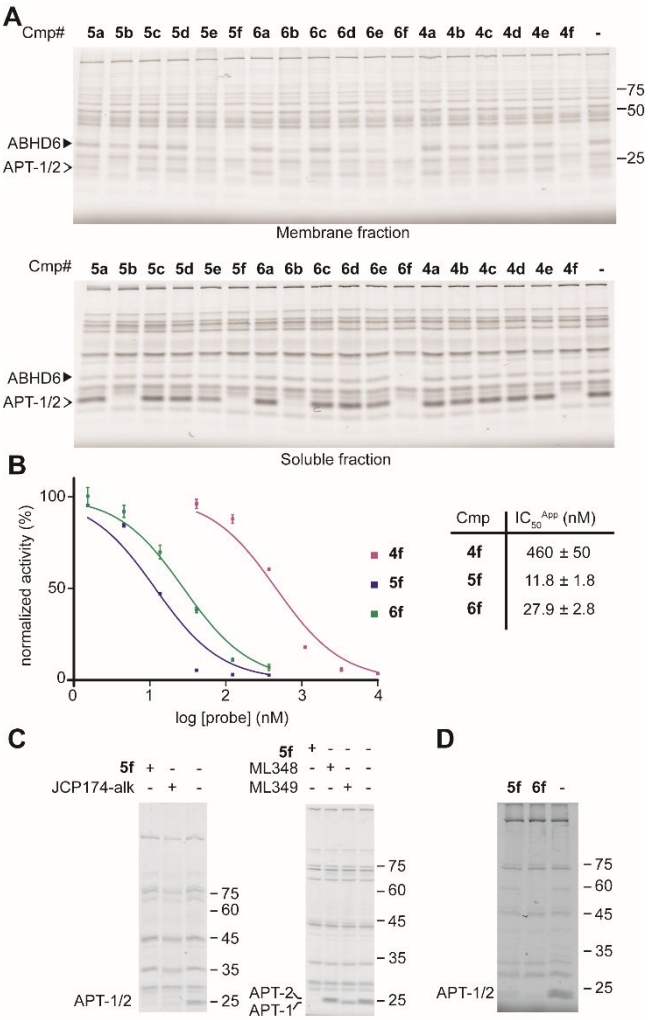

Figure 2. Screening of SH ABP library for inhibition by competitive ABPP. (A) Fluorescent gels of competitive ABPP in the membrane fraction (upper) or soluble fraction (lower) of mouse brain lysates. Pretreatment of lysate with the indicated probe was followed by measurement of residual SH activity with FP-Rh. (B) Apparent IC_{50} curves were determined by competitive ABPP of serial dilutions, followed by quantification using gel band densitometry. (C) Competitive ABPP in mouse brain lysate (soluble fraction) with known APT1/2 inhibitor JCP-174-alk (left panel) or APT1-selective inhibitor ML348 and APT2-selective inhibitor ML349 (right panel) in comparison with compound **5f**. Residual SH activity in treated tissue lysates was measured by incubation with FP-Rh. (D) Inhibition of APT1/2 by compounds **5f** and **6f** in live A431 cells. After treatment, compounds were washed out, and residual SH activity in cell lysates was detected with FP-Rh.

Direct profiling of probe targets. To show the utility of the synthesized molecules as novel, highly selective ABPs against SHs, probes were applied in a labeling experiment using copper-catalyzed azide alkyne cycloaddition (CuAAC) with an alkyne-functionalized fluorophore. At 1 μM concentration, all three probes showed strong labeling of the APT-1/2 band, and this labeling was even retained at 100 nM concentration for probes **5f** and **6f** (Figure 3A-B). Interestingly, a few other targets besides the APT-1/2 gel bands were revealed in this direct labeling experiment (indicated with a red asterisk, Figure 3A-B), which were not detected in the competitive ABPP experiment that made use of FP-Rh. This illustrates that not all probe targets overlap with general SH probe FP-rhodamine. Specifically, probe **6f** showed strong labeling of a soluble protein at 30 kDa (Figure 3A) and membrane proteins at 35 and 55 kDa (Figure 3B). Probes **4f** and **5f** both showed reactivity towards a different membrane protein at 33 kDa at 1 μM. However SDS-PAGE analysis of **5f** at 100 nM concentration did not show any other labeling than APT-1/2 (Figure 3B, right panel)..

Previously reported proteomics based assessments of the targets of FP-rhodamine in brain lysates show that it labels APT-1/2 as targets at 25 kD.[24] Given our competitive based ABPP results with FP-rhodamine, we suspected these as being the targets of our NHS-carbamate and triazole ureaprobes. To confirm that these close-running gel bands correspond to APT-1/2, we incubated mouse brain lysates with **5f** or **6f**, followed by click labelling of the probe-enzyme complexes with a trifunctional TAMRA-biotin-alkyne detection tag. This tag allowed affinity-based enrichment of the probe hits on streptavidin-coated beads, followed by both fluorescent visualization (Figure 3C, upper panels, full gels in Figure S5) as well as Western blot analysis (Figure 3C; lower panels). The detected bands with anti-APT-1 and anti-APT-2 antibodies in the samples treated with probe, but not in dmso controls unequivocally reveal the identity of the probe target.

Model of probe binding. To gain insight into the binding mode of the two most active compounds **5f** and **6f** towards their targets, we performed covalent docking using the flexible sidechain methods of Autodock 4.2.[28 29] In a crystal structure of APT-1 with a bound palmitate

molecule (PDB code: 6QGS), both probes overlay well with this substrate (Figure 3D-E) and occupy a long, hydrophobic channel, which is also the binding site of the recently reported, reversible APT-1 inhibitor ML348 (Figure S6).[30] The Inp residue of the most potent probe **5f** seems locked between hydrophobic residues F73, I75, W145 and L176, whereas its peptoid Phe moiety binds into a pocket created by the residues F73, I75, I76 and the alkyl chain of E84 (Figure 3D). Although the slightly less active probe **6f** does not have the peptoid Phe, it may compensate for this by a stacking interaction of the benzoyl group in its backbone with W145, whereas its piperidine ring has similar hydrophobic interactions as the Inp in probe **5f** with L30, I75, W145 and L176 (Figure 3E).

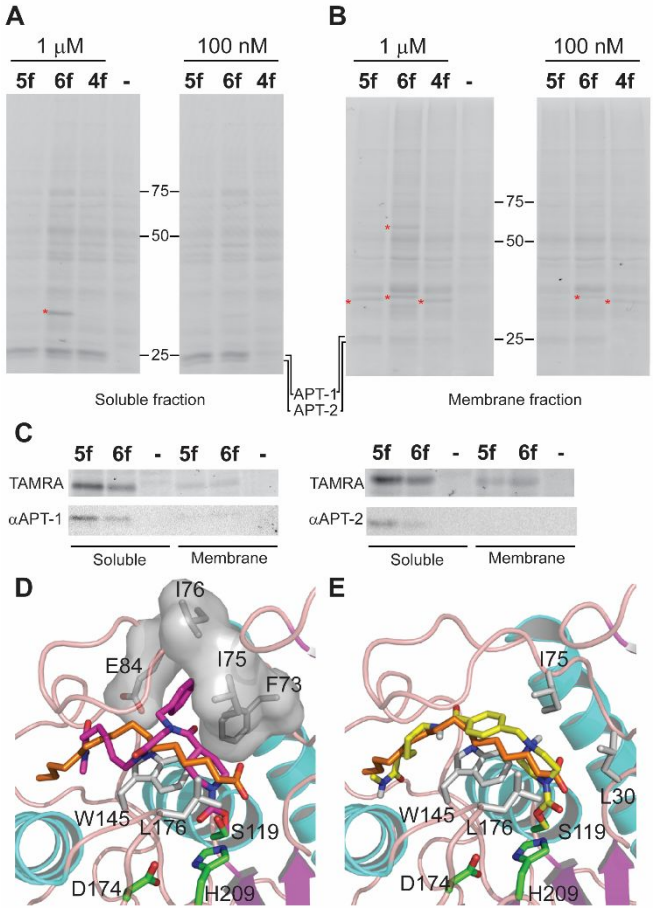

Figure 3. Covalent interaction with APT-1/2. (A) Labeling of a soluble fraction of mouse brain lysate with probes **4f-6f**, followed by click chemistry with a TAMRA-alkyne derivative shows selective detection of the ATP-1/2 gel bands. DMSO control (-) shows click background. Other protein targets than APT-1/2 are indicated by a *. (B) Same as (A) but in the membrane fraction of mouse brain lysate. (C) After click chemistry with a trifunctional biotin-TAMRA-alkyne tag

and enrichment on streptavidin beads, fluorescent detection (upper panels) confirms target engagement of the probes, while detection by anti-APT-1 or anti-APT-2 antibodies (lower panels) confirms target identity. Note that the targets in the membrane fraction were very low abundant and led to very weak bands. Full fluorescent gels in Figure S5. (D) Covalent docking of **5f** in a crystal structure of APT-1 (PDB code: 6QGS). Protein in cartoon format with α-helices in cyan, β-sheets in magenta and random coil in pink. A co-crystallized palmitate is shown in orange sticks, whereas **5f** is shown in magenta. Active site residues are depicted in green, whereas interacting residues are shown in white. Picture rendered with PyMol.[31] (E) Covalent docking of **6f** (in yellow) overlayed with co-crystallized palmitate (in orange) in a crystal structure of APT-1.

Conclusions

In conclusion, we report synthetic procedures for a full on-resin synthesis of SH chemical probes compatible with six different types of serine-reactive electrophiles. Using this procedure, we constructed a library of ABPs by combining the electrophiles with three different recognition elements consisting of an aromatic unit and a piperidine or piperazine moiety. Evaluation of these compounds in a serine-hydrolase rich mouse brain lysate revealed activity of five of these compounds against protein depalmitoylases APT-1 and APT-2, with triazole urea **5f** showing nanomolar potency and excellent selectivity. The structure-activity relationship from this work may provide new information on pharmacophores for the design of drug-like APT-1/2 inhibitors and the in silico docking presented here provides a plausible model of the binding mode of these compounds. Compared with other recently reported inhibitors and probes for APT1/2,[26 27] the compounds presented here can be readily synthesized on solid support and allow for easy future optimization by medicinal chemistry studies.

We expect that the novel selective ABPs **5f** and **6f** resulting from this work will find application in the study of APT1/2-mediated protein depalmitoylation. Furthermore, the synthetic procedures reported in this work may be automated in future work and facilitate more rapid development of SH inhibitors and ABPs by library synthesis on solid support. Since many

SHs are still poorly characterized, we expect that this will open the door to functional studies of these.

Experimental section

General materials and methods

All starting materials for chemical reactions were purchased from commercial suppliers and used without purification. All solvents were of synthesis grade or higher. Progress of solution phase reactions was monitored by TLC on pre-coated 0.20 mm thick ALUGRAM® TLC sheets (silicagel-60 with UV indicator) using UV light and/or staining with cerium ammonium molybdate or ninhydrin followed by heating. Nuclear magnetic resonance spectra were recorded on a Bruker Ultrashield™ 400 or 600 MHz NMR Spectrometer. Chemical shifts are reported in ppm relative to the residual solvent peak. LC-MS spectra were recorded on a Prominence Ultra-fast Liquid Chromatography system (Shimadzu) using a Waters X-bridge 2.1 mm C18 column with a gradient of 5%-80% acetonitrile in water (with 0.1% formic acid) over 22 min. HPLC purification was performed on a Prominence Ultra-fast Liquid Chromatography system (Shimadzu) using a Waters X-bridge 150 mm C18 prep column with a gradient of acetonitrile in water (with 0.1% trifluoroacetic acid) over 32 min. Purity >95% of all final compounds was assessed by integration of LC chromatograms.

Solid phase chemistry procedures

Fmoc protected Rink amide resin (1.35 g, 0.74 mmol/g) was treated with 20% piperidine in DMF for 5 min to swell the resin and deprotect the Fmoc group. Next, the resin was washed three times with DMF. All following Fmoc deprotections were performed according to this procedure.

Backbone synthesis

Method 1. Fmoc-L-Lys(N_3)-OH was coupled to 1 mmol of deprotected rink amide resin by adding amino acid (1.5 eq.), HBTU (1.5 eq.) and DIPEA (3 eq.) in 4 mL of DMF to the resin

and incubating for 4 hours at room temperature. After this and each following coupling, the resin was washed three times with DMF and three times with DCM. After deprotection, Fmoc-6-aminohexanoic acid was coupled by adding amino acid (2 eq.), HBTU (2 eq.) and DIPEA (4 eq.) in 4 mL DMF to the resin and incubating overnight at room temperature.

Recognition element synthesis

After synthesis of the peptide backbone, the resin was divided into portions of 100 µmol on which the different recognition elements were formed. Peptide bonds in recognition elements were formed with the corresponding (amino)acid (3 eq.), DIC (3 eq.) and HOBt (3 eq.) in 1.5 mL DMF overnight at room temperature unless stated otherwise.

Method 2.1. Phe-peptoid was formed by coupling Br-acetic acid to the peptide backbone under standard SPPS conditions and subsequent substitution with benzylamine (20 eq.) and DIPEA (10 eq.) in 1.5 mL DMF per 100 µmol overnight at room temperature. Next, Fmoc-Isonipecotic acid was coupled using standard SPPS conditions.

Method 2.2. 4-Bromomethyl phenylacetic acid (3 eq.) was coupled to the peptide backbone with PyBrOP (3 eq.) and DIPEA (6 eq.) in 1.5 mL DMF per 100 µmol overnight at room temperature. Subsequently, the bromide was substituted for piperazine (20 eq.) using DIPEA (10 eq.) in 1.5 mL DMF overnight at room temperature.

Method 2.3. Fmoc-L-Phe-OH was coupled to the peptide backbone using standard SPPS conditions, followed by coupling of Fmoc-Isonipecotic acid under standard SPPS conditions.

Warhead coupling

After synthesis of the recognition elements, the resins were divided into portions of 10 µmol for coupling of the warheads.

Method 3.1.: Synthesis of diphenyl phosphoramidates. Resin (1 eq.) was swollen in 0.5 mL DMF per 10 µmol of resin, to which DIEA (5 eq.) and Diphenylphosphoryl chloride (5 eq.) were added. Reactions were shaken overnight at room temperature and checked for completion

using LC/MS. After completion, the resin was washed three times with DMF and twice with DCM. Probes were then cleaved from the resin by using a 95:2.5:2.5 mixture of TFA:TIS:water.

Method 3.2.: Synthesis of hydroxysuccinimidylcarbamates. Resin (1 eq.) was swollen in 0.5 mL DMF per 10 μmol of resin, to which DIEA (5 eq.) and Disuccinimidylcarbonate (3 eq.) were added. Reactions were shaken overnight at room temperature and checked for completion using LC/MS. After completion, the resin was washed three times with DMF and twice with DCM. Probes were then cleaved from the resin by using a 95:2.5:2.5 mixture of TFA:TIS:water.

Method 3.3.: Synthesis of aminopyridine ureas. Resin (1 eq.) was swollen in 0.5 mL DMF per 10 μmol of resin, to which were added DIPEA (5 eq.) and phenyl 2-pyridinylcarbamate (3 eq.; synthesized from 2-aminopyridine and phenyl chloroformate according to the method described by Swanson et al.[32] and isolated in 29% yield). Reactions were shaken overnight at room temperature and checked for completion using LC/MS. After completion, the resin was washed three times with DMF and twice with DCM. Probes were then cleaved from the resin by using a 95:2.5:2.5 mixture of TFA:TIS:water.

Method 3.4.: Synthesis of phenylcarbamates: Resin (1 eq.) was swollen in 0.5 mL DMF per 10 μmol of resin, to which DIEA (10 eq.) and Phenyl chloroformate (10 eq.) were added. Reactions were shaken overnight at room temperature and checked for completion using LC/MS. After completion, the resin was washed three times with DMF and twice with DCM. Probes were then cleaved from the resin by using a 95:2.5:2.5 mixture of TFA:TIS:water.

Method 3.5.: Synthesis of *p*-nitrophenylcarbamates: Resin (1 eq.) was swollen in 0.5 mL DMF per 10 μmol of resin, to which DIEA (10 eq.) and *p*-nitrophenyl chloroformate (10 eq.) were added. Reactions were shaken overnight at room temperature and checked for completion using LC/MS. After completion, the resin was washed three times with DMF and twice with DCM. Probes were then cleaved from the resin by using a 95:2.5:2.5 mixture of TFA:TIS:water.

Method 3.6.: Synthesis of triazole ureas: Resin (1 eq.) was swollen in 1 mL dry DCM per 10 μmol of resin, to which DIEA (15 eq.) and triphosgene (3 eq.) were added. Reactions were shaken at room temperature for 30 min, after which the cartridge was drained into a solution of 10% NaOH in water. The resin was washed three times with dry DCM, which was drained

into a 10%NaOH solution. Next, the resin was resuspended in 1 mL dry DCM, to which 10 equivalents of 1*H*-1,2,3-triazole was added. Reactions were shaken overnight at room temperature and checked for completion using LC/MS. After completion, the resin was washed three times with DCM. Probes were then cleaved from the resin by using a 95:2.5:2.5 mixture of TFA:TIS:water. Note that with this on resin synthesis, the N1-isomer of the triazole ureas was formed (Figure S7).

_N_-(Diphenylphosphoryl)-isonipecotyl-L-phenylalanyl-6-aminohexanoyl-L-ε-azidolysine amide (4a)

Probe **4a** was synthesized using subsequently methods 1, 2.3 and 3.1 and purified using HPLC. The product was obtained as a white powder. (1.84 mg, yield = 23.7%) HRMS (MALDI-TOF): m/z calcd. for $C_{39}H_{51}N_8O_7P$ $[M+H]^+$ 775.3691, found: 775.3412.

_N_-(Succinimidyloxycarbonyl)-isonipecotyl-L-phenylalanyl-6-aminohexanoyl-L-ε-azidolysine amide (4b)

Probe **4b** was synthesized using subsequently methods 1, 2.3 and 3.2 and purified using HPLC. The product was obtained as a white powder. (3.31 mg, yield = 48.4%) HRMS (MALDI-TOF): m/z calcd. for $C_{32}H_{45}N_9O_8$ $[M+H]^+$ 684.3464, found: 684.3167.

_N_-(2-aminopyridin-2-yl-carbonyl)-isonipecotyl-L-phenylalanyl-6-aminohexanoyl-L-ε-azidolysine amide (4c)

Probe **4c** was synthesized using subsequently methods 1, 2.3 and 3.3 and purified using HPLC. The product was obtained as a white powder. (2.99 mg, yield = 45.1%) HRMS (MALDI-TOF): m/z calcd. for $C_{34}H_{46}N_{10}O_5$ $[M+H]^+$ 663.3725, found: 663.3597.

_N_-(Phenyloxycarbonyl)-isonipecotyl-L-phenylalanyl-6-aminohexanoyl-L-ε-azidolysine amide (4d)

Probe **4d** was synthesized using subsequently methods 1, 2.3 and 3.4 and purified using HPLC. The product was obtained as a white powder. (3.37 mg, yield = 50.8%) HRMS (MALDI-TOF): m/z calcd. for $C_{34}H_{46}N_8O_6$ $[M+H]^+$ 663.3613, found: 663.3211.

***N*-(4-Nitrophenyloxycarbonyl)-isonipecotyl-L-phenylalanyl-6-aminohexanoyl-L-ε-azidolysine amide (4e)**

Probe **4e** was synthesized using subsequently methods 1, 2.3 and 3.5 and purified using HPLC. The product was obtained as a white powder. (1.93 mg, yield = 27.3%) HRMS (MALDI-TOF): m/z calcd. for $C_{34}H_{45}N_9O_8$ $[M+H]^+$ 708.3464, found: 708.3064.

***N*-(1H-1,2,3-triazol-1-yl-carbonyl)-isonipecotyl-L-phenylalanyl-6-aminohexanoyl-L-ε-azidolysine amide (4f)**

Probe **4f** was synthesized using subsequently methods 1, 2.3 and 3.6 and purified using HPLC. The product was obtained as a white powder. (0.36 mg, yield = 5.6%) HRMS (MALDI-TOF): m/z calcd. for $C_{30}H_{43}N_{11}O_5$ $[M+H]^+$ 638.3521, found: 638.3790.

***N*-(Diphenylphosphoryl)-isonipecotyl-(*N*-benzyl)glycyl-6-aminohexanoyl-L-ε-azidolysine amide (5a)**

Probe **5a** was synthesized using subsequently methods 1, 2.1 and 3.1 and purified using HPLC. The product was obtained as a white powder. (0.33 mg, yield = 4.3%) HRMS (MALDI-TOF): m/z calcd. for $C_{39}H_{51}N_8O_7P$ $[M+H]^+$ 775.3691, found: 775.3742.

***N*-(Succinimidyloxycarbonyl)-isonipecotyl-(*N*-benzyl)glycyl-6-aminohexanoyl-L-ε-azidolysine amide (5b)**

Probe **5b** was synthesized using subsequently methods 1, 2.1 and 3.2 and purified using HPLC. The product was obtained as a white powder. (1.29 mg, yield = 18.9%) HRMS (MALDI-TOF): m/z calcd. for $C_{32}H_{45}N_9O_8$ $[M+H]^+$ 684.3391, found: 684.3342.

_N_-(2-aminopyridin-2-yl-carbonyl)-isonipecotyl-(_N_-benzyl)glycyl-6-aminohexanoyl-L-ε-azidolysine amide (5c)

Probe **5c** was synthesized using subsequently methods 1, 2.1 and 3.3 and purified using HPLC. The product was obtained as a white powder. (2.82 mg, yield = 42.5%) HRMS (MALDI-TOF): m/z calcd. for $C_{34}H_{46}N_8O_6$ $[M+H]^+$ 663.37301, found: 663.3648.

_N_-(Phenyloxycarbonyl)-isonipecotyl-(_N_-benzyl)glycyl-6-aminohexanoyl-L-ε-azidolysine amide (5d)

Probe **5d** was synthesized using subsequently methods 1, 2.1 and 3.4 and purified using HPLC. The product was obtained as a white powder. (2.80 mg, yield = 42.2%) HRMS (MALDI-TOF): m/z calcd. for $C_{33}H_{46}N_{10}O_5$ $[M+H]^+$ 663.3619, found: 663.3772.

_N_-(4-Nitrophenyloxycarbonyl)-isonipecotyl-(_N_-benzyl)glycyl-6-aminohexanoyl-L-ε-azidolysine amide (5e)

Probe **5e** was synthesized using subsequently methods 1, 2.1 and 3.5 and purified using HPLC. The product was obtained as a white powder. (2.97 mg, yield = 41.9%) HRMS (MALDI-TOF): m/z calcd. for $C_{34}H_{45}N_9O_8$ $[M+H]^+$ 708.3469, found: 708.3151.

_N_-(1H-1,2,3-triazol-1-yl-carbonyl)-isonipecotyl-(_N_-benzyl)glycyl-6-aminohexanoyl-L-ε-azidolysine amide (5f)

Probe **5f** was synthesized using subsequently methods 1, 2.1 and 3.6 and purified using HPLC. The product was obtained as a white powder. (1.06 mg, yield = 16.6%) HRMS (MALDI-TOF): m/z calcd. for $C_{30}H_{43}N_{11}O_5$ $[M+Na]^+$ 660.3346, found: 660.2908.

_N_-(Diphenylphosphoryl)-4-(piperazinyl-methyl)-benzoyl-6-aminohexanoyl-L-ε-azidolysine amide (6a)

Probe **6a** was synthesized using subsequently methods 1, 2.2 and 3.1 and purified using HPLC. The product was obtained as a white powder. (0.93 mg, yield = 12.9%) HRMS (MALDI-TOF): m/z calcd. for $C_{36}H_{47}N_8O_6P$ $[M+H]^+$ 719.3435, found: 719.3851.

***N*-(Succinimidyloxycarbonyl)-4-(piperazinyl-methyl)-benzoyl-6-aminohexanoyl-L-ε-azidolysine amide (6b)**

Probe **6b** was synthesized using subsequently methods 1, 2.2 and 3.2 and purified using HPLC. The product was obtained as a white powder. (0.93 mg, yield = 12.9%) HRMS (MALDI-TOF): m/z calcd. for $C_{29}H_{41}N_9O_7$ $[M+H]^+$ 628.3201, found: 628.3192.

***N*-(2-aminopyridin-2-yl-carbonyl)-4-(piperazinyl-methyl)-benzoyl-6-aminohexanoyl-L-ε-azidolysine amide (6c)**

Probe **6c** was synthesized using subsequently methods 1, 2.2 and 3.3 and purified using HPLC. The product was obtained as a white powder. (0.69 mg, yield = 11.4%) HRMS (MALDI-TOF): m/z calcd. for $C_{31}H_{42}N_8O_5$ $[M+H]^+$ 607.3351, found: 607.3222.

***N*-(Phenyloxycarbonyl)-4-(piperazinyl-methyl)-benzoyl-6-aminohexanoyl-L-ε-azidolysine amide (6d)**

Probe **6d** was synthesized using subsequently methods 1, 2.2 and 3.4 and purified using HPLC. The product was obtained as a white powder. (0.49 mg, yield = 8.1%) HRMS (MALDI-TOF): m/z calcd. for $C_{30}H_{42}N_{10}O_4$ $[M+H]^+$ 607.3463, found: 607.3647.

***N*-(4-Nitrophenyloxycarbonyl)-4-(piperazinyl-methyl)-benzoyl-6-aminohexanoyl-L-ε-azidolysine amide (6e)**

Probe **6e** was synthesized using subsequently methods 1, 2.2 and 3.5 and purified using HPLC. The product was obtained as a white powder. (0.63 mg, yield = 9.7%) HRMS (MALDI-TOF): m/z calcd. for $C_{31}H_{41}N_9O_7$ $[M+H]^+$ 652.3202, found: 652.2670.

***N*-(1H-1,2,3-triazol-1-yl-carbonyl)-4-(piperazinyl-methyl)-benzoyl-6-aminohexanoyl-L-ε-azidolysine amide (6f)**

Probe **6f** was synthesized using subsequently methods 1, 2.2 and 3.6 and purified using HPLC. The product was obtained as a white powder. (0.34 mg, yield = 5.8%) HRMS (MALDI-TOF): m/z calcd. for $C_{27}H_{39}N_{11}O_4$ $[M+H]^+$ 582.3259, found: 582.3079.

Preparation of tissue lysates

Mouse brains were thawed on ice, after which the hemispheres were separated using a razor blade and cut into small pieces. The pieces were collected in a Dounce homogenizer and homogenized on ice using 1.5 mL cold (4 °C) lysis buffer (20 mM HEPES, 2 mM DTT, 1 mM $MgCl_2$, 25 U/mL DNAse I, pH 7.2) until thorough lysis of the organ was visually assessed. After homogenization, the suspension was collected into Eppendorf tubes and the Dounce homogenizer was rinsed twice with small aliquots of lysis buffer, which were added to these tubes. The suspension was centrifuged (2500 g, 3 min, 4°C) to remove cell debris. The supernatant was carefully pipetted and transferred to an ultracentrifuge tube. The debris was resuspended in 0.25 mL lysis buffer and centirfuged again using the same procedure. The supernatant was added to the ultracentrifuge tubes, which were then spun in an ultracentrifuge (100,000 g, 45 min, 4 °C, Beckman Optima™ TLX, TLA 120.2 rotor). The supernatant (= cytosolic protein fraction) was collected and the pellet (= membrane protein fraction) was suspended in 1.5 mL storage buffer (20 mM HEPES, 2 mM DTT, pH 7.2). Protein concentrations were determined using BCA assay on a Spectramax ID3 platereader. Aliquots were snap frozen in liquid nitrogen and stored at -80 °C until use.

Competition of probes with FP-rhodamine

30 μL of cytosolic or membrane fraction of mouse brain lysate (1 mg/mL) was incubated for 1 h at room temperature with 0.3 μL of a stock solution of probe (10 mM, DMSO) or 0.3 μL

DMSO. Then 0.3 μL FP-rhodamine (100 μM, DMSO) was added to each sample and the samples were incubated for another hour. Next, 10 μL 4x sample buffer was added to the samples, which were subsequently boiled at 95 °C for 2 minutes. Samples were resolved by SDS-PAGE on 12% acrylamide gels and visualized by measuring in-gel fluorescence on a Typhoon FLA 9500 scanner with excitation at 532 nm and detection at 568 nm with the photomultiplier set at 900 V. Patterns of probe-treated samples were compared with an FP-rhodamine treated control sample. Compounds that led to full disappearance of gel bands were considered hits.

Comparison of 5f with JCP-174 alk

30 μL of cytosolic or membrane fraction of mouse brain lysate (1 mg/mL) was incubated for 1 h at room temperature with either 0.3 μL of a stock solution of probe **5f** (10 μM, DMSO), 0.3 μL of a stock solution of JCP-174 alk (1 mM, DMSO) or 0.3 μL DMSO. Then 0.3 μL FP-rhodamine (100 μM, DMSO) was added to each sample and the samples were incubated for 1 hour at room temperature. Next, 10 μL 4x sample buffer was added to the samples, which were subsequently boiled at 95 °C for 2 minutes. Samples were resolved by SDS-PAGE on 12% acrylamide gels and visualized by measuring in-gel fluorescence on a Typhoon FLA 9500 scanner with settings as described above.

Comparison of 5f with ML-348 and ML-349

30 μL of cytosolic fraction of mouse brain lysate (1 mg/mL) was incubated for 1 h at room temperature with either 0.3 μL of a stock solution of probe **5f** (10 μM, DMSO), 0.3 μL of a stock solution of ML-348 or ML-349 (50 mM, DMSO) or 0.3 μL DMSO. Then 0.3 μL FP-rhodamine (100 μM, DMSO) was added to each sample and the samples were incubated for 5 minutes at room temperature. Next, 10 μL 4x sample buffer was added to the samples, which were subsequently boiled at 95 °C for 2 minutes. Samples were resolved by SDS-PAGE on 12%

acrylamide gels and visualized by measuring in-gel fluorescence on a Typhoon FLA 9500 scanner with settings as described above.

Cell permeability assay in A431 cells

A431 cells were seeded at 300,000 cells per well into a 6-well plate and allowed to adhere overnight. The media was refreshed with 1 mL DMEM (with 10% FBS and pen/strep), spiked with either 1 µL **5f** or **6f** (1 mM, DMSO) or 1 µL DMSO for 2h at 37 °C. Next, the medium was aspirated and the cells were washed three times with PBS (5 min). Lysates were prepared by incubating cells in 150 µL lysis buffer (20 mM HEPES, 150 mM NaCl, 2 mM DTT, 25 U/mL Benzonase, 0.5% NP-40, pH 7.2) before scraping cells. Lysates were centrifuged (13000 g, 5 min, room temperature) to pellet debris, after which the supernatant was pipetted off. Protein concentrations of all samples were measured using a BCA assay, and normalized to 2.39 mg/mL with storage buffer (20 mM HEPES, 2 mM DTT, pH 7.2). 90 µL of each sample was incubated with either 0.9 µL FP-rhodamine (DMSO, 100 µM) or 0.9 µL DMSO at room temperature for 1 hour. Next, 30 µL 4x sample buffer was added to the samples, which were subsequently boiled at 95 °C for 2 minutes. Samples were resolved by SDS-PAGE on 12% acrylamide gels and visualized by measuring in-gel fluorescence on a Typhoon FLA 9500 scanner with settings as described above.

IC_{50} determination

Apparent IC_{50} values were measured by using six different compound concentrations in a 1:3 serial dilution, starting at a highest concentration of 30 µM or 370 nM, depending on the potency of the compound.. To this end 30 µL of cytosolic or membrane fraction of mouse brain lysate (1 mg/mL) was incubated for 1 h at room temperature with 0.3 µL of a 100x stock solution of probe in DMSO. Then, 0.3 µL FP-rhodamine (100 µM, DMSO) was added to each sample and the samples were incubated for another hour. Next 10 µL 4x sample buffer was added to the samples, which were subsequently boiled at 95 °C for 2 minutes. Samples were resolved

by SDS-PAGE on 12% acrylamide gels and visualized by in-gel fluorescence measuring on a Typhoon scanner as for the initial screening. Remaining enzyme activity was determined by measuring the integrated optical gel band intensity using ImageJ software. Values were normalized to the FP-rhodamine labeled control sample without inhibitor, which was set at 100% activity. IC_{50} values were determined from a dose-response curve generated in GraphPad Prism.

Direct labelling of probe targets

30 μL of cytosolic or membrane fraction of mouse brain lysate (1 mg/mL) was incubated for 1 h with 0.3 μL of a 100x stock solution of the appropriate concentration. Next, 0.5 μL TAMRA-alkyne (1.5 mM in DMSO), 0.3 μL THPTA (5 mM in 4:1 t-BuOH: DMSO), 0.6 μL sodium ascorbate (50 mM in water) and 0.6 μL $CuSO_4$ (50 mM in water) were added to each sample and the samples were incubated 1 h at room temperature. Afterwards, 10 μL of 4x sample buffer was added to the samples, which were subsequently boiled at 95 °C for 2 minutes. Samples were resolved on an SDS-PAGE 12% acrylamide gel and visualized by in-gel fluorescence measuring on a Typhoon scanner.

Western blot against APT-1/2

Mouse brain lysates (90 μL, 1 mg/mL of either cytosolic or membrane fraction) were treated for 1 h with 1 μM probe (from a 100x dmso stock) or a corresponding amount of dmso (control sample). All samples were subsequently treated with 1,5 μL tritag (TAMRA-Lys(biotin)-NH-propyne; 1.5 mM in DMSO), 0.9 μL THPTA (5 mM in water), 1.8 μL $CuSO_4$ (50 mM in water) and 1.8 μL sodium ascorbate (50 mM in water), after which they were incubated for another hour at room temperature. Next, 360 μL of cold acetone (-80 °C) was added to each sample to precipitate proteins and eliminate residual click reagents. The samples were incubated at -20 °C for 30 minutes to ensure efficient protein precipitation, after which they were spun down

using a microcentrifuge at max speed. The supernatant was discarded, another 360 μL cold acetone was added to the pellet of the samples and the procedure was repeated once more. Protein pellets were then redissolved in 90 μL PBS with 2% SDS. Next, SDS was diluted with steps of 90 μL to a final concentration of 0.4% SDS. Then, 30 μL of Ultralink Streptavidin resin slurry was added to each sample to pull down all biotin-labeled proteins. To this end, all samples were incubated on a thermomixer (1h, 1200 rpm, 25 °C). Afterwards, the samples were spun down using a microcentrifuge at full speed.

The supernatant was carefully pippeted from the beads, after which the beads were washed with 120 μL of 0.1% SDS in PBS, subsequently with 120 μL of 1M NaCl, then with 120 μL 1M urea, then with 120 μL PBS and finally with 120 μL MilliQ water. After each washing step, the samples were spun down using a microcentrifuge at full speed and the supernatant was discarded. The beads were resuspended in 120 μL sample buffer and boiled for 10 minutes to release the proteins from the beads. Samples were then resolved on a 12% acrylamide gel using SDS-PAGE.

A fluorescent image of the gels was made (Typhoon scanner), after which the proteins were transferred onto nitrocellulose membranes. Both membranes were incubated for 1h with 3% milk/PBST. The milk was discarded and one of the gels was incubated overnight with 15 mL anti-APT-1 antibody Ab 91606 (0.5 μg/mL in PBST), whereas the other membrane was incubated overnight with 15 mL anti-APT-2 antibody Ab 151578 (0.5 μg/mL in PBST). The antibody-solutions were then decanted and the membranes washed four times with PBST. Next, both membranes were incubated with anti-rabbit HRP antibody (0.2 μg/mL in PBST) for 1h. Afterwards, the membranes were washed four times with PBST and incubated with SuperSignal West Pico Plus chemiluminescent substrate (Life Technologies) just prior to development using a BioRad ChemiDoc imaging system.

Covalent docking

The different probes were drawn in Chemdraw professional 15.1, converted to a pdb file using Chem3D 15.1 and converted into a PDBQT by AutoDockTools 1.5.6. Probes were attached with their carbonyl function (with elimination of the leaving group) to the side chain of residue S119 of APT-1 (PDB code: 6QGS, from which water molecules and the palmitate ligand were removed), using the provided script at the autodock website (see for download: http://autodock.scripps.edu/resources/covalentdocking) with a slight modification. Molecules were then docked according to the flexible side chain method of AutoDock 4.2, as described by Bianco et al.[29] The connected molecules were treated as a fully flexible side chain. The binding site was covered by preparing a 60 × 76 × 70 size grid box with grid spacing of 0.375 Å and the center at 7.837, 127.491, 18.586.

Associated content

Supporting information

The Supporting Information is available free of charge at https://pubs.acs.org/

Additional synthetic procedures, Supporting Figures S1-S7, copies of NMR spectra and HPLC purity data, coomassie stains of gels

Coordinates of docked probes

Molecular formula strings

Funding

We acknowledge financial support from Research Foundation Flanders FWO (project number G0E3617N), the Ministerium für Kultur und Wissenschaft des Landes Nordrhein-Westfalen, the Regierende Bürgermeister von Berlin–inkl. Wissenschaft und Forschung, and the Bundesministerium für Bildung und Forschung.

Acknowledgments

The authors thank Luc Baudemprez for recording NMR spectra and Rita Derua for HRMS.

Abbreviations

ABDH6, α,β-hydrolose domain containing protein 6; ABP, activity-based probe; ABPP, activity-based protein profiling; APT-1/2, acyl protein thioesterase-1/2; CuAAC, copper(I)-catalyzed azide alkyne cycloaddition; DAGL, diacylglycerol lipase; FP, fluorophosphonate; MAGL, monoacylglycerol lipase; NHS, *N*-hydroxysuccinimide; SH, serine hydrolase

References

1. Cravatt, B. F.; Wright, A. T.; Kozarich, J. W., Activity-based protein profiling: from enzyme chemistry to proteomic chemistry. *Annu. Rev. Biochem.* **2008,** 77, 383-414.

2. Sadaghiani, A. M.; Verhelst, S. H. L.; Bogyo, M., Tagging and detection strategies for activity-based proteomics. *Curr. Opin. Chem. Biol.* **2007,** 11, (1), 20-8.

3. Liu, Y. S.; Patricelli, M. P.; Cravatt, B. F., Activity-based protein profiling: The serine hydrolases. *Proc. Natl. Acad. Sci. USA* **1999,** 96, (26), 14694-14699.

4. Patricelli, M. P.; Giang, D. K.; Stamp, L. M.; Burbaum, J. J., Direct visualization of serine hydrolase activities in complex proteomes using fluorescent active site-directed probes. *Proteomics* **2001,** 1, (9), 1067-71.

5. Jessani, N.; Liu, Y. S.; Humphrey, M.; Cravatt, B. F., Enzyme activity profiles of the secreted and membrane proteome that depict cancer cell invasiveness. *Proc. Natl. Acad. Sci. USA* **2002,** 99, (16), 10335-10340.

6. Bachovchin, D. A.; Cravatt, B. F., The pharmacological landscape and therapeutic potential of serine hydrolases. *Nat. Rev. Drug. Discov.* **2012,** 11, (1), 52-68.

7. Savinainen, J. R.; Saario, S. M.; Laitinen, J. T., The serine hydrolases MAGL, ABHD6 and ABHD12 as guardians of 2-arachidonoylglycerol signalling through cannabinoid receptors. *Acta Physiol.* **2012,** 204, (2), 267-76.

8. Davda, D.; Martin, B. R., Acyl protein thioesterase inhibitors as probes of dynamic S-palmitoylation. *Med. Chem. Comm.* **2014,** 5, (3), 268-276.

9. Sontag, J. M.; Nunbhakdi-Craig, V.; Mitterhuber, M.; Ogris, E.; Sontag, E., Regulation of protein phosphatase 2A methylation by LCMT1 and PME-1 plays a critical role in differentiation of neuroblastoma cells. *J. Neurochem.* **2010,** 115, (6), 1455-65.

10. Bachovchin, D. A.; Ji, T.; Li, W.; Simon, G. M.; Blankman, J. L.; Adibekian, A.; Hoover, H.; Niessen, S.; Cravatt, B. F., Superfamily-wide portrait of serine hydrolase inhibition achieved by library-versus-library screening. *Proc. Natl. Acad. Sci. USA* **2010,** 107, (49), 20941-20946.

11. Cheng, R.; Mori, W.; Ma, L.; Alhouayek, M.; Hatori, A.; Zhang, Y.; Ogasawara, D.; Yuan, G.; Chen, Z.; Zhang, X.; Shi, H.; Yamasaki, T.; Xie, L.; Kumata, K.; Fujinaga, M.; Nagai, Y.; Minamimoto, T.; Svensson, M.; Wang, L.; Du, Y.; Ondrechen, M. J.; Vasdev, N.; Cravatt, B. F.; Fowler, C.; Zhang, M. R.; Liang, S. H., In Vitro and in Vivo Evaluation of (11)C-Labeled Azetidinecarboxylates for Imaging Monoacylglycerol Lipase by PET Imaging Studies. *J. Med. Chem.* **2018,** 61, (6), 2278-2291.

12. Chen, Z.; Mori, W.; Fu, H.; Schafroth, M. A.; Hatori, A.; Shao, T.; Zhang, G.; Van, R. S.; Zhang, Y.; Hu, K.; Fujinaga, M.; Wang, L.; Belov, V.; Ogasawara, D.; Giffenig, P.; Deng, X.; Rong, J.; Yu, Q.; Zhang, X.; Papisov, M. I.; Shao, Y.; Collier, T. L.; Ma, J. A.; Cravatt, B. F.; Josephson, L.; Zhang, M. R.; Liang, S. H., Design, Synthesis, and Evaluation of (18)F-Labeled Monoacylglycerol Lipase Inhibitors as Novel Positron Emission Tomography Probes. *J. Med. Chem.* **2019,** 62, (19), 8866-8872.

13. Chang, J. W.; Moellering, R. E.; Cravatt, B. F., An activity-based imaging probe for the integral membrane hydrolase KIAA1363. *Angew. Chem. Int. Ed. Engl.* **2012,** 51, (4), 966-70.

14. van Rooden, E. J.; Kohsiek, M.; Kreekel, R.; van Esbroeck, A. C. M.; van den Nieuwendijk, A.; Janssen, A. P. A.; van den Berg, R.; Overkleeft, H. S.; van der Stelt, M., Design and Synthesis of Quenched Activity-based Probes for Diacylglycerol Lipase and alpha,beta-Hydrolase Domain Containing Protein 6. *Chem. Asian J.* **2018,** 13, (22), 3491-3500.

15. van Rooden, E. J.; Kreekel, R.; Hansen, T.; Janssen, A. P. A.; van Esbroeck, A. C. M.; den Dulk, H.; van den Berg, R.; Codee, J. D. C.; van der Stelt, M., Two-step activity-based protein profiling of diacylglycerol lipase. *Org. Biomol. Chem.* **2018,** 16, (29), 5250-5253.

16. Chang, J. W.; Cognetta, A. B., 3rd; Niphakis, M. J.; Cravatt, B. F., Proteome-wide reactivity profiling identifies diverse carbamate chemotypes tuned for serine hydrolase inhibition. *ACS Chem. Biol.* **2013,** 8, (7), 1590-9.

17. Haedke, U. R.; Frommel, S. C.; Hansen, F.; Hahne, H.; Kuster, B.; Bogyo, M.; Verhelst, S. H., Phosphoramidates as novel activity-based probes for serine proteases. *ChemBioChem* **2014,** 15, (8), 1106-10.

18. Otrubova, K.; Srinivasan, V.; Boger, D. L., Discovery libraries targeting the major enzyme classes: the serine hydrolases. *Bioorg. Med. Chem. Lett.* **2014,** 24, (16), 3807-13.

19. Adibekian, A.; Martin, B. R.; Wang, C.; Hsu, K. L.; Bachovchin, D. A.; Niessen, S.; Hoover, H.; Cravatt, B. F., Click-generated triazole ureas as ultrapotent in vivo-active serine hydrolase inhibitors. *Nat. Chem. Biol.* **2011,** 7, (7), 469-78.

20. Long, J. Z.; Jin, X.; Adibekian, A.; Li, W.; Cravatt, B. F., Characterization of tunable piperidine and piperazine carbamates as inhibitors of endocannabinoid hydrolases. *J. Med. Chem.* **2010,** 53, (4), 1830-42.

21. Aaltonen, N.; Savinainen, J. R.; Ribas, C. R.; Ronkko, J.; Kuusisto, A.; Korhonen, J.; Navia-Paldanius, D.; Hayrinen, J.; Takabe, P.; Kasnanen, H.; Pantsar, T.; Laitinen, T.; Lehtonen, M.; Pasonen-Seppanen, S.; Poso, A.; Nevalainen, T.; Laitinen, J. T., Piperazine and piperidine triazole ureas as ultrapotent and highly selective inhibitors of monoacylglycerol lipase. *Chem. Biol.* **2013,** 20, (3), 379-90.

22. Lamani, M.; Malamas, M. S.; Farah, S. I.; Shukla, V. G.; Almeida, M. F.; Weerts, C. M.; Anderson, J.; Wood, J. T.; Farizatto, K. L. G.; Bahr, B. A.; Makriyannis, A., Piperidine and piperazine inhibitors of fatty acid amide hydrolase targeting excitotoxic pathology. *Bioorg. Med. Chem.* **2019,** 27, (23), 115096.

23. Baggelaar, M. P.; van Esbroeck, A. C.; van Rooden, E. J.; Florea, B. I.; Overkleeft, H. S.; Marsicano, G.; Chaouloff, F.; van der Stelt, M., Chemical Proteomics Maps Brain Region Specific Activity of Endocannabinoid Hydrolases. *ACS Chem. Biol.* **2017,** 12, (3), 852-861.

24. Blankman, J. L.; Simon, G. M.; Cravatt, B. F., A comprehensive profile of brain enzymes that hydrolyze the endocannabinoid 2-arachidonoylglycerol. *Chem. Biol.* **2007,** 14, (12), 1347-56.

25. van Rooden, E. J.; van Esbroeck, A. C. M.; Baggelaar, M. P.; Deng, H.; Florea, B. I.; Marques, A. R. A.; Ottenhoff, R.; Boot, R. G.; Overkleeft, H. S.; Aerts, J.; van der Stelt, M., Chemical Proteomic Analysis of Serine Hydrolase Activity in Niemann-Pick Type C Mouse Brain. *Front. Neurosci.* **2018,** 12, 440.

26. Adibekian, A.; Martin, B. R.; Chang, J. W.; Hsu, K. L.; Tsuboi, K.; Bachovchin, D. A.; Speers, A. E.; Brown, S. J.; Spicer, T.; Fernandez-Vega, V.; Ferguson, J.; Hodder, P. S.; Rosen, H.; Cravatt, B. F., Confirming target engagement for reversible inhibitors in vivo by kinetically tuned activity-based probes. *J. Am. Chem. Soc.* **2012,** 134, (25), 10345-10348.

27. Garland, M.; Schulze, C. J.; Foe, I. T.; van der Linden, W. A.; Child, M. A.; Bogyo, M., Development of an activity-based probe for acyl-protein thioesterases. *PLoS One* **2018,** 13, (1), e0190255.

28. Morris, G. M.; Huey, R.; Lindstrom, W.; Sanner, M. F.; Belew, R. K.; Goodsell, D. S.; Olson, A. J., AutoDock4 and AutoDockTools4: Automated docking with selective receptor flexibility. *J. Comput. Chem.* **2009,** 30, (16), 2785-91.

29. Bianco, G.; Forli, S.; Goodsell, D. S.; Olson, A. J., Covalent docking using autodock: Two-point attractor and flexible side chain methods. *Protein Sci.* **2016,** 25, (1), 295-301.

30. Won, S. J.; Davda, D.; Labby, K. J.; Hwang, S. Y.; Pricer, R.; Majmudar, J. D.; Armacost, K. A.; Rodriguez, L. A.; Rodriguez, C. L.; Chong, F. S.; Torossian, K. A.; Palakurthi, J.; Hur, E. S.; Meagher, J. L.; Brooks, C. L., 3rd; Stuckey, J. A.; Martin, B. R., Molecular Mechanism for Isoform-Selective Inhibition of Acyl Protein Thioesterases 1 and 2 (APT1 and APT2). *ACS Chem. Biol.* **2016,** 11, (12), 3374-3382.

31. Delano, W. L., The Pymol Molecular Graphics Systems **2002** (http://www.pymol.org).

32. Swanson, D. M.; Dubin, A. E.; Shah, C.; Nasser, N.; Chang, L.; Dax, S. L.; Jetter, M.; Breitenbucher, J. G.; Liu, C.; Mazur, C.; Lord, B.; Gonzales, L.; Hoey, K.; Rizzolio, M.; Bogenstaetter, M.; Codd, E. E.; Lee, D. H.; Zhang, S. P.; Chaplan, S. R.; Carruthers, N. I., Identification and biological evaluation of 4-(3-trifluoromethylpyridin-2-yl)piperazine-1-carboxylic acid (5-trifluoromethylpyridin-2-yl)amide, a high affinity TRPV1 (VR1) vanilloid receptor antagonist. *J. Med. Chem.* **2005,** 48, (6), 1857-72.

Table of Contents Graphic

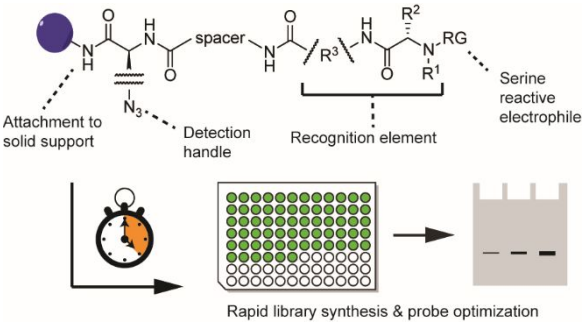

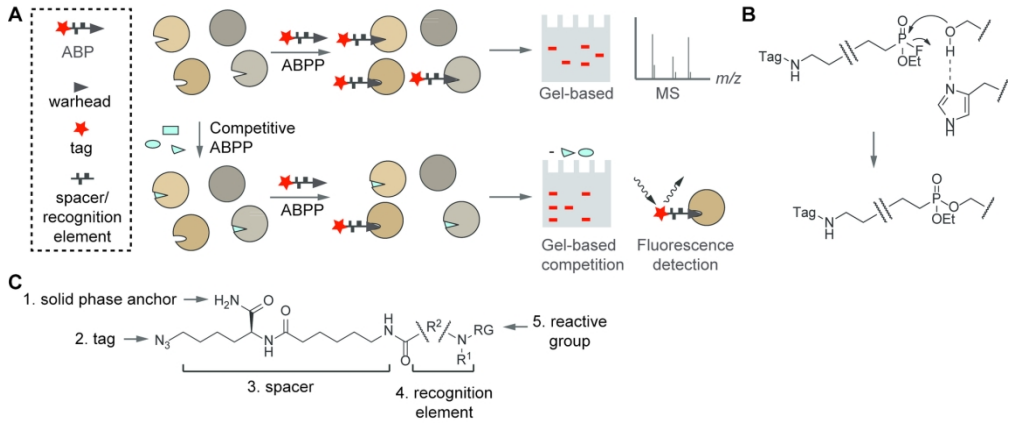

Figure 1. ABPP and ABPs. (A) Left (boxed): ABPs generally consist of three elements: a reactive electrophile as warhead that engages in a mechanism-based reaction with the active site nucleophiles of the target, a tag that allows detection and a spacer and/or recognition element to prevent a steric clash of the tag in the active site and to influence the selectivity of the probe. Right: ABPP allows the tagging of active enzyme targets in a complex proteome, such as a cell lysate, whole cell or in vivo setting, followed by various types of read-out. Inhibitor evaluation in complex proteomes may be done by 'competitive ABPP', in which the proteome is first treated with a potential inhibitor before incubation with the ABP. Disappearance of gel bands in SDS-PAGE will then reveal inhibitor selectivity. (B) Structure of fluorophosphonate-based probes and the mechanism of reaction with serine hydrolases: the active site serine side chain, activated by hydrogen bonding to a histidine residue, engages in a mechanism-based reaction and results in a stable, covalent phosphonate ester probe-protein complex. (C) A modular design of SH ABPs for construction on solid support.

173x72mm (300 x 300 DPI)

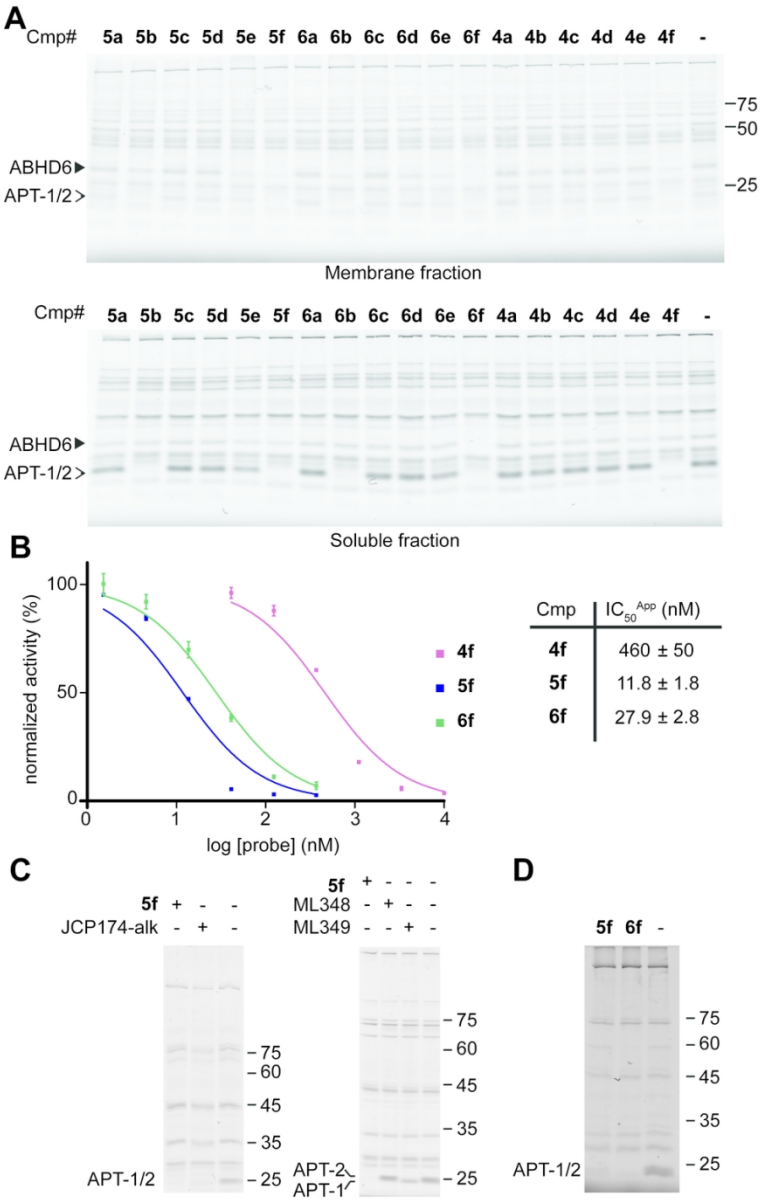

Figure 2. Screening of SH ABP library for inhibition by competitive ABPP. (A) Fluorescent gels of competitive ABPP in the membrane fraction (upper) or soluble fraction (lower) of mouse brain lysates. Pretreatment of lysate with the indicated probe was followed by measurement of residual SH activity with FP-Rh. (B) Apparent IC50 curves were determined by competitive ABPP of serial dilutions, followed by quantification using gel band densitometry. (C) Competitive ABPP in mouse brain lysate (soluble fraction) with known APT1/2 inhibitor JCP-174-alk (left panel) or APT1-selective inhibitor ML348 and APT2-selective inhibitor ML349 (right panel) in comparison with compound 5f. Residual SH activity in treated tissue lysates was measured by incubation with FP-Rh. (D) Inhibition of APT1/2 by compounds 5f and 6f in live A431 cells. After treatment, compounds were washed out, and residual SH activity in cell lysates was detected with FP-Rh.

84x134mm (300 x 300 DPI)

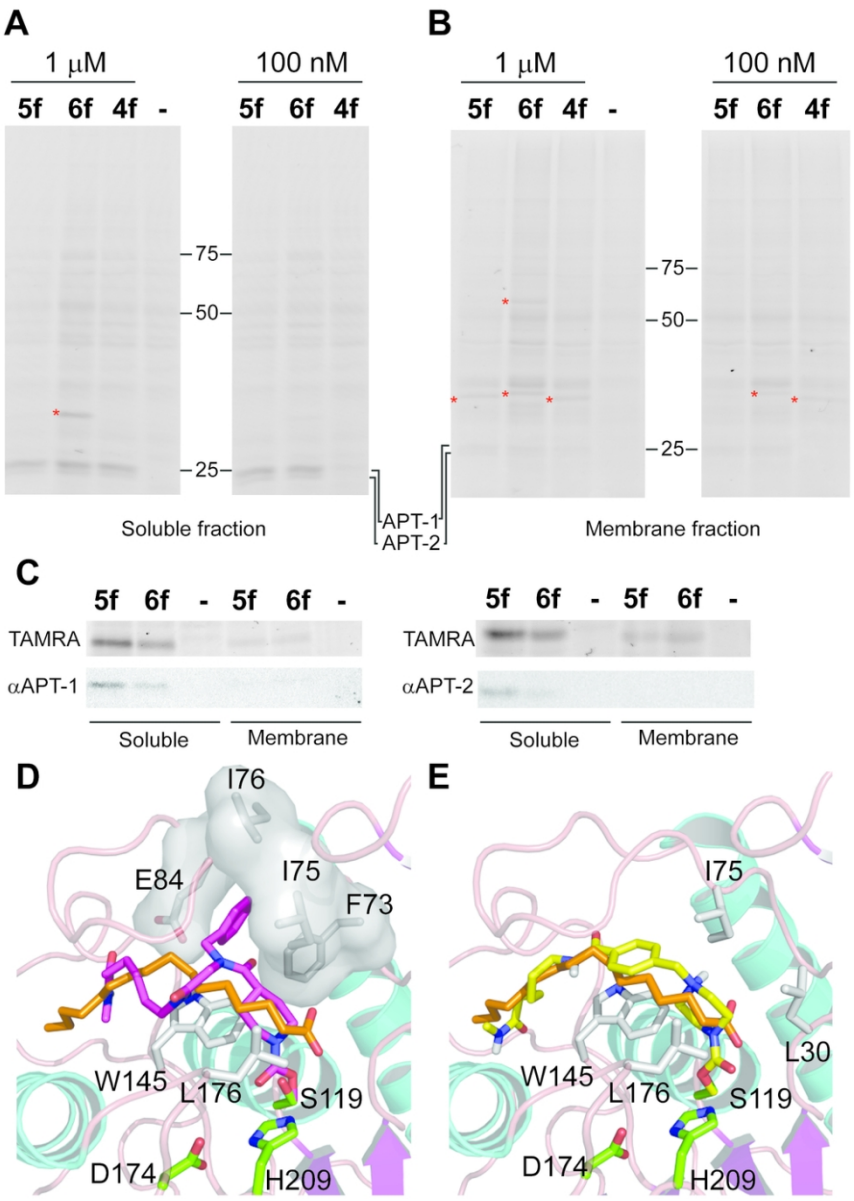

Figure 3. Covalent interaction with APT-1/2. (A) Labeling of a soluble fraction of mouse brain lysate with probes 4f-6f, followed by click chemistry with a TAMRA-alkyne derivative shows selective detection of the ATP-1/2 gel bands. DMSO control (-) shows click background. Other protein targets than APT-1/2 are indicated by a *. (B) Same as (A) but in the membrane fraction of mouse brain lysate. (C) After click chemistry with a trifunctional biotin-TAMRA-alkyne tag and enrichment on streptavidin beads, fluorescent detection (upper panels) confirms target engagement of the probes, while detection by anti-APT-1 or anti-APT-2 antibodies (lower panels) confirms target identity. Note that the targets in the membrane fraction were very low abundant and led to very weak bands. Full fluorescent gels in Figure S5. (D) Covalent docking of 5f in a crystal structure of APT-1 (PDB code: 6QGS). Protein in cartoon format with □-helices in cyan, □-sheets in magenta and random coil in pink. A co-crystallized palmitate is shown in orange sticks, whereas 5f is shown in magenta. Active site residues are depicted in green, whereas interacting residues are shown in white. Picture rendered with PyMol.31 (E) Covalent docking of 6f (in yellow) overlayed with co-crystallized palmitate (in orange) in a crystal structure of APT-1.

85x120mm (300 x 300 DPI)

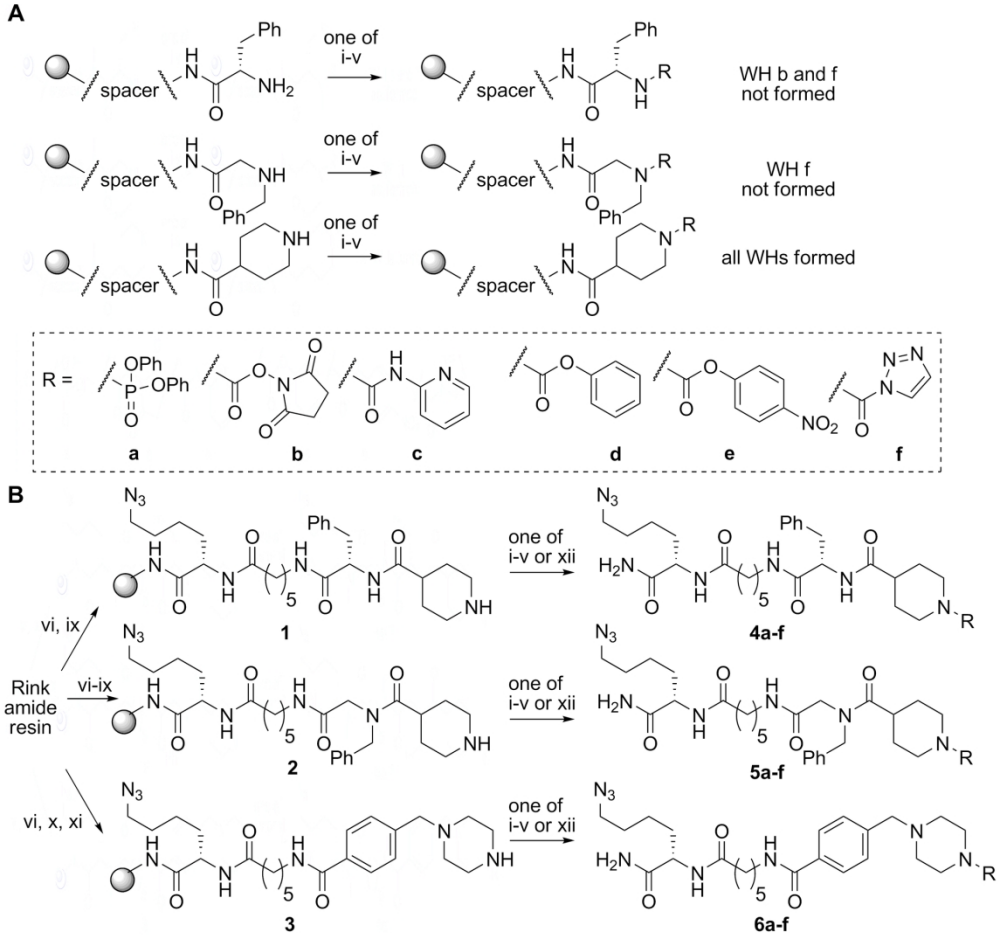

Scheme 1. Synthesis of mix-and-match SH ABP libraries.a

a (A) On resin coupling of warheads to different types of amines. Reagents and conditions: (i) Diphenylphosphoryl chloride, DIEA, DCM. (ii) Disuccinimidylcarbonate, DIEA, DCM. (iii) 2-aminopyridinyl phenyl carbamate, DIEA, DCM. (iv) phenyl chloroformate, DIEA, DCM. (v) 1. Triphosgene, DIEA, DCM, 30 minutes; 2. 1H-1,2,3-triazole, DIEA, DCM. (B) Library synthesis towards compounds 4a-6f. (vi) SPPS elongation by 1. DMF/piperidine 4/1, 15 min; 2. Fmoc-aa-OH, HBTU, DIEA, DMF. (vii) 1. DMF/piperidine 4/1, 5 min; 2. Bromoacetic acid, DIC, HOBt, DMF. (viii) Benzylamine, DIEA, DMF. (ix) Fmoc-Inp-OH, DIC, HOBt, DMF. (x) p-Bromomethylbenzoic acid, PyBrOP, DIEA, DMF. (xi) Piperazine, DMF. (xii) 4-nitrophenyl chloroformate, DIEA, DCM.

180x169mm (300 x 300 DPI)